# Crystal Structures of Rat Vitamin D Receptor Bound to Adamantyl Vitamin D Analogs: Structural Basis for Vitamin D Receptor Antagonism and Partial Agonism

Makoto Nakabayashi,[†] Sachiko Yamada,*[,†,‡] Nobuko Yoshimoto,[†] Takashi Tanaka,[†] Miharu Igarashi,[†] Teikichi Ikura,[†] Nobutoshi Ito,[†] Makoto Makishima,[‡] Hiroaki Tokiwa,[§] Hector F. DeLuca,[||] and Masato Shimizu[†]

*School of Biomedical Science and Institute of Biomaterials and Bioengineering, Tokyo Medical and Dental University, 2-3-10 Kanda-Surugadai, Chiyoda-ku, Tokyo 101-0062, School of Medicine, Nihon University, 30-1 Ohyaguchikami-machi, Itabashi-ku, Tokyo 173-0086, Department of Chemistry, Faculty of Science, Rikkyo University, 3-34-1 Nishi-Ikebukuro, Toshima-ku, Tokyo 171-8501, and Department of Biochemistry, University of Wisconsin-Madison, Madison, Wisconsin 53706-1544*

*Received April 19, 2008*

The X-ray crystal structures of the rat VDR ligand-binding domain complexed with 19-norvitamin D compounds that contain an adamantyl substituent at the side-chain terminus, **2a** (ADTT), **2b** (ADNY), and **2c** (ADMI4) and a coactivator peptide derived from DRIP205 are reported. These compounds show a series of partial agonistic (10−75% efficacy)/antagonistic activities. All of these complexed receptors are crystallized in the canonical active conformation, regardless of their activity profiles. The bulky adamantyl side chain does not crowd helix 12 but protrudes into the gap formed by helix 11, loop 11−12, helix 3, and loop 6−7, thereby widening the ligand binding pocket. We suggest that these structural changes destabilize the active protein conformation and reduce its contribution to equilibrium among the active and inactive conformations. The coactivator peptide traps the minor active conformation, and the equilibrium shifts to the active conformation. As a result, these ligands show partial agonistic activities.

## Introduction

The hormonally active vitamin D metabolite $1,25(OH)_2D_3$ expresses its function by binding to the vitamin D receptor (VDR[a], NR1I1),[1−7] which is a ligand-regulated transcription factor and a member of the nuclear receptor (NR) superfamily.[8,9] The VDR plays physiological roles in the regulation of the mineral homeostasis and proliferation, the differentiation, and the immune response of cells.[10,11] Active vitamin $D_3$ and some potent synthetic analogs have been used clinically to treat calcium and bone disorders such as osteoporosis and the skin disorder psoriasis.[10,11] However, despite some degree of target selectivity, the further development of vitamin D analogs as medicines for the treatment of malignant tumors and autoimmune disorders and for selective bone formation has been limited because of the adverse effect of hypercalcemia.[12−14] The development of VDR modulators with selectivity at the tissue level (i.e., SVDRM) to overcome this limitation has been awaited, and for this purpose, a search for VDR partial agonists/antagonists is of great interest.[59]

Selective receptor modulators (SRM) exhibit agonistic or antagonistic activity in a cell and tissue context-dependent manner.[15] In NRs without ligands (apo), both the active and the inactive conformations are in equilibrium. With a bound agonist (holo), NRs predominantly adopt the active conformation to which coactivators[16] are recruited, and chromatin remodeling[17] and transactivation follow. When accommodating an antagonist, the receptors preferentially adopt inactive conformations that interact with corepressors,[16] and transactivation is kept silent. When binding a SRM, NRs adopt both active and inactive conformations and therefore have the potential to interact with either coactivators or corepressors and exert partial activity. Therefore, the activity of SRM-bound receptors depends on the relative expression of coactivators and corepressors in a given cell environment.

In the NR field, many antagonists and partial agonists have been developed as clinical medicines. For example, hydroxytamoxifen (OHT)[18] and raloxifene (RAL)[19] have been developed as selective estrogen receptor (ER) modulators (SERMs),[15] the mineralocorticoid receptor (MR) antagonist spironolactone[20] has been developed as an antihypertensive agent, and androgen receptor (AR) antagonists such as flutamide[21] and bicalutamide[22] have been developed for the treatment of prostate cancer. The X-ray crystal structures of these steroid hormone receptors complexed with their antagonistic and partially agonistic ligands have been determined.[23−30] These crystallographic studies have revealed that the conformations of antagonist- and partial-agonist-bound NRs are varied whereas agonist-bound NRs adopt the same canonical active conformation.

In the VDR field, a few vitamin D analogs that have antagonistic activity, partial agonistic activity, or both have been reported, including compounds that contain a bulky alkoxycarbonyl group at the side-chain terminus, such as **5**,[31−34] compounds that have a methylene lactone structure in the side chain, such as **6**,[34−36] and their analogs,[37−39] and nonsteroidal VDR modulators (Figure 1).[40] However, the X-ray crystal structure of VDR complexed with an antagonistic ligand has never been reported, although a number of agonist complexes have been determined.[41−49] We have designed and synthesized vitamin D derivatives that have the bulky adamantyl (AD) substituent at the terminus of side chains of various lengths[50−53] (Figure 1). These compounds have partial agonistic activity

* To whom correspondence should be addressed. Tel: +81 42 664 1629. Fax: +81 42 664 1629. E-mail: yamada.vd@image.ocn.ne.jp.
† Tokyo Medical and Dental University.
‡ Nihon University.
§ Rikkyo University.
|| University of Wisconsin-Madison.

[a] Abbreviations: VDR, vitamin D receptor; NR, nuclear receptor; SVDRM, selective vitamin D receptor modulator; ER, estrogen receptor; MR, mineralocorticoid receptor; AR, androgen receptor; SRM, selective receptor modulator; OHT, hydroxytamoxifen; RAL, raloxifene; SERM, selective estrogen receptor modulator; AD, adamantane; LBD, ligand binding domain; LBP, ligand binding pocket; GEN, genistein; THC, tetrahydrochrysene; 2D ASMA, two-dimensional alanine scanning mutational analysis.

10.1021/jm8004477 CCC: $40.75 © 2008 American Chemical Society
Published on Web 08/19/2008

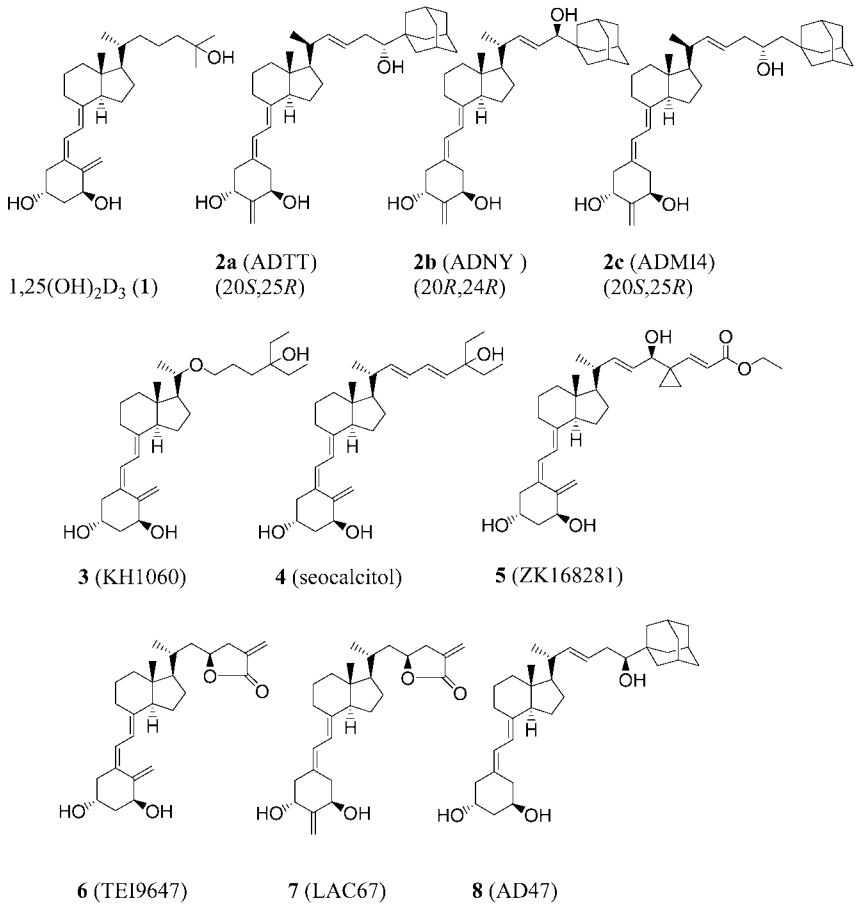


**Figure 1.** Structures of vitamin D analogs discussed in this article.

(10−75% efficacy), antagonistic activity, or both. In the present study, we determined the X-ray crystal structures of the rat VDR ligand-binding domain (LBD) complexed with AD 19-norvitamin D compounds with various side-chain lengths and various activity profiles (25-AD-25-hydroxyl (**2a**), 24-AD-24-hydroxyl (**2b**), and 26-AD-25-hydroxyl (**2c**) (Figure 1)) and an LXXLL-containing coactivator peptide. In all of these ternary complexes, the VDR was found to adopt the canonical active conformation of NR, regardless of their activity profiles. These results provide a structural basis for VDR antagonism and partial agonism for the first time as well as supporting evidence of the general molecular mechanism of SRM that was previously suggested.[15]

## Results

**Synthesis.** We designed AD 19-nor-2-methylenevitamin D compounds as candidates for potential VDR partial agonists and antagonists because (1) the rigid, bulky side chain with the AD moiety together with the 22-double would interfere with H12 in the active conformation and (2) the 19-nor-2-methylene A-ring motif that was introduced by DeLuca's group[54,55] promises a high VDR affinity that is important for antagonistic activity. It is also advantageous that the 19-norvitamin D moiety is chemically stable and easy to synthesize.

New AD compounds, **2a** and **2b**, were synthesized by the methods shown in Scheme 1, which are essentially the same as the method that was previously reported for the synthesis of 26-AD-19-nor-vitamin D compounds including **2c**.[51] The C22 secosteroid unit and side-chain fragment were combined by the Julia coupling reaction. In the synthesis of **2a**, the C22 aldehyde (**8**) was combined with side-chain sulfone **5d**, whereas in the synthesis of **2b**, the reversed pair of C22 sulfone (**13b**) and side-chain aldehyde (**7**) was employed. The reductive elimination of the hydroxysulfone group via the acetate, followed by the deprotection of the hydroxyl groups, afforded the desired compounds.

**Crystal Structures.** The crystals of rVDR LBD (116−423, Δ165−211) were grown in the presence of a ligand (AD compounds **2a**−**2c** or **1**) and a peptide containing the LXXLL motif that was derived from coactivator DRIP 205. The complexes of rVDR LBD with AD compounds **2a** and **2b** were readily crystallized in space group *C*2 and were refined to resolutions of 1.70 and 2.10 Å, respectively. In contrast, the complex of **2c** was crystallized rather slowly (resolution 2.35 Å), which suggests that the ligand was accommodated in the LBP with its very minor conformation. The crystal data are given in the Supporting Information.

The overall folds of rVDR LBD bound to **2a**, **2b**, and **2c** (Figures 2A−C) are identical to each other and to those of the VDR complexes of the natural hormone (**1**)[41,43] and its agonistic analogs.[42,44−49] Contrary to our expectation, all three of these complexes adopted the canonical active conformation of the NR LBD, and the coactivator peptide bound to the coactivator recognition surface (AF-2 surface). The VDR complexes of AD compounds (**2a**, **2b**, and **2c**) are aligned at Cα atoms with the complex of **1**, which was crystallized in this study from the same recombinant rVDR LBD, with average root-mean-square (rms) deviations of 0.344, 0.262, and 0.385 Å, respectively. The ligands are accommodated in the ligand binding pockets (LBP), which are significantly widened at the tip of the side chains compared with the complex with the natural hormone (**1**). The volumes of the LBP with **1**, **2a**, **2b**, and **2c** are 942, 1040, 1092, and 1102 Å$^3$, respectively. The LBP of the rVDR

**Scheme 1**[a]

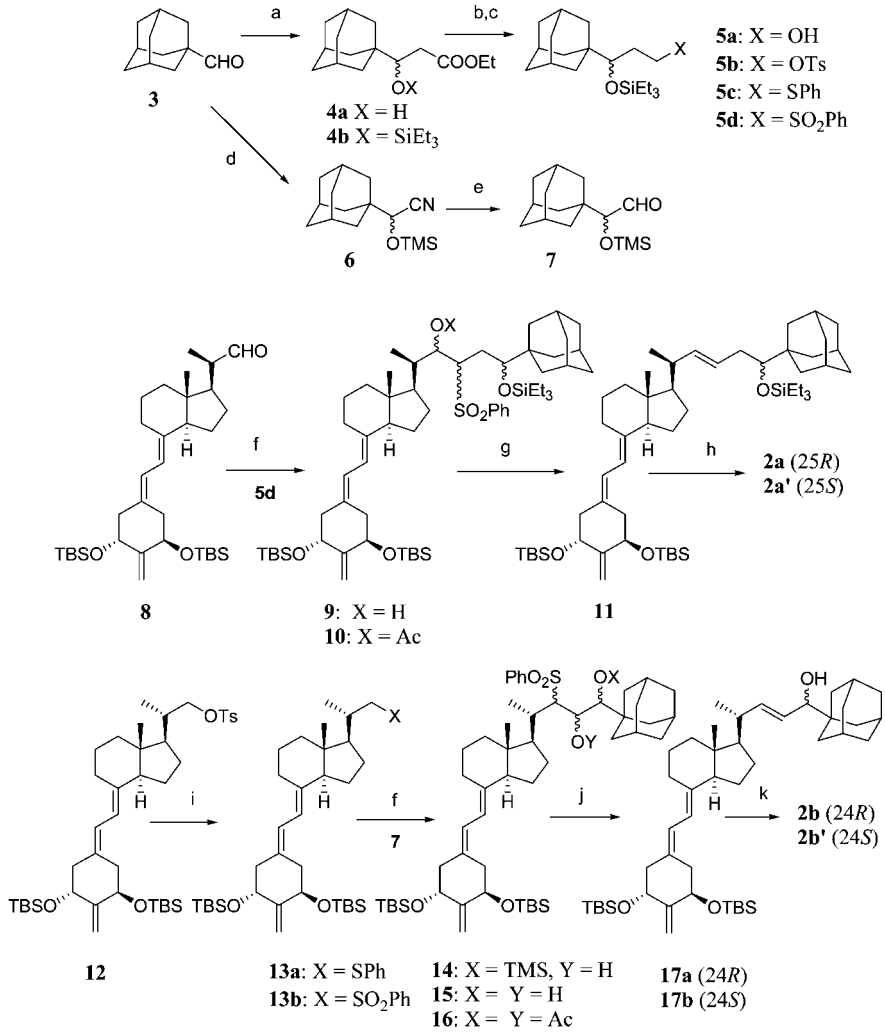


[a] Reagents and conditions: (a) Zn, $BrCH_2COOEt$, benzene, reflux (72.9%); $Et_3SiCl$, imidazole, DMF (94.2%). (b) DIBAL-H, toluene, −78 °C (98.3%). (c) TsCl, pyridine, 0 °C (91%); PhSH, t-BuOK, DMF, 0 °C (83%); *m*-CPBA, $CH_2Cl_2$, 0 °C (94%). (d) TMSCN, $ZnI_2$, $CH_2Cl_2$, 0 °C (75.3%). (e) DIBAL-H, toluene/$CH_2Cl_2$, 0 °C (68.7%). (f) LDA, THF, −20 °C. (g) $Ac_2O$, DMAP, pyridine; Na−Hg, $Na_2HPO_4$ (37.4% from **8**). (h) CSA, MeOH (80.5%). (i) PhSH, t-BuOK, DMF, 0 °C (99.8%); $Na_2WO_4 \cdot 2H_2O$, 30% $H_2O_2$, $CH_2Cl_2$/MeOH (3:5), 0 °C ∼room temperature (65%). (j) AcOH/THF/$H_2O$; $Ac_2O$, DMAP, pyridine; Na−Hg, $Na_2HPO_4$ (34% from **13b**). (k) *n*-$Bu_4NF$, DMF/THF (98.8%).

LBD complexed with **2a** is shown in Figure 2D in comparison with that of the $1,25(OH)_2D_3$ complex. The ligand **2a** (space-filling model) is accommodated in its LBP but protrudes from that of the $1,25(OH)_2D_3$ complex.

**Complex with 2a.** 25-Adamantyl-25-hydroxyl compound **2a** shows very potent partial agonistic activity, antagonistic activity, or both: [51] VDR affinity, ∼75% that of natural hormone **1**; transactivation, $EC_{50} = 10^{-9}$ M, 15% efficacy compared to that of **1**; and inhibition of the action of **1**, $IC_{50} = 3 \times 10^{-9}$ M. Regardless of **2a**'s potent antagonistic activity, the VDR complex of **2a** adopts the transcriptionally active conformation. This active conformation complex is conceivably a minor component in the equilibrium with major inactive conformations and was trapped by the LXXLL peptide and was crystallized out. In accord with the high VDR affinity, ligand **2a** is anchored strongly by three pairs of hydrogen bonds at its three hydroxyl groups as natural hormone **1**: 1α-OH, Ser233 and Arg270 (2.81 and 2.98 Å, respectively); 3β-OH, Tyr143 and Ser274 (2.80 and 2.86 Å, respectively); 25-OH, His301 and His 393 (2.82 and 2.71 Å, respectively) (Figure 3A). The Cα rms deviations of individual residues are shown in Figure 2E. (≤0.24, 0.25−0.44, 0.45−0.74, 0.75−1.04, and ≥1.05 Å are yellow, orange, red, purple, and black, respectively.) Large rms deviations are found in the loop parts. Specifically, Cα rms deviations of loop 11−12 are most significant. The Cα rms deviations are also significant at Ala148−Pro155 (the loop following H1), His367−Gln374 (loop 10−11), and L303−Lys311 (H7). However, the rms deviations of functionally important residues such as those on H12 and the signature region (highly conserved sequences among the NR family consisting of the C-terminus of H3, loop 3−4, and H4) are not noticeable. As described above, the LBP is widened around the part that is surrounded by the C-terminus of H11, loop 11−12, and the N-terminus of H3 (Figures 2D). Here, the side-chain conformations of three Leu residues, 223 (H3), 400 (H11), and 410 (loop 11−12), differ significantly from those of the $1,25(OH)_2D_3$ complex (Figure 3D): rms deviations, Leu 223 Cδ$_1$ and Cδ$_2$ (2.79 and 2.53 Å, respectively); Leu400 Cγ, Cδ$_1$, and Cδ$_2$ (2.12, 3.11, and 3.21 Å, respectively); Leu410 Cδ$_1$ and Cδ$_2$ (2.52 and 2.67 Å, respectively). We have shown by alanine scanning mutational analysis (ASMA)[50] that these residues are important in the folding of the active conformation of the hVDR LBD. The widening of the LBP here may explain why compound **2a** shows antagonistic activity. This weakens the interactions among the secondary structures here and destabilizes the active conformation. It has been reported that the volume of the hVDR

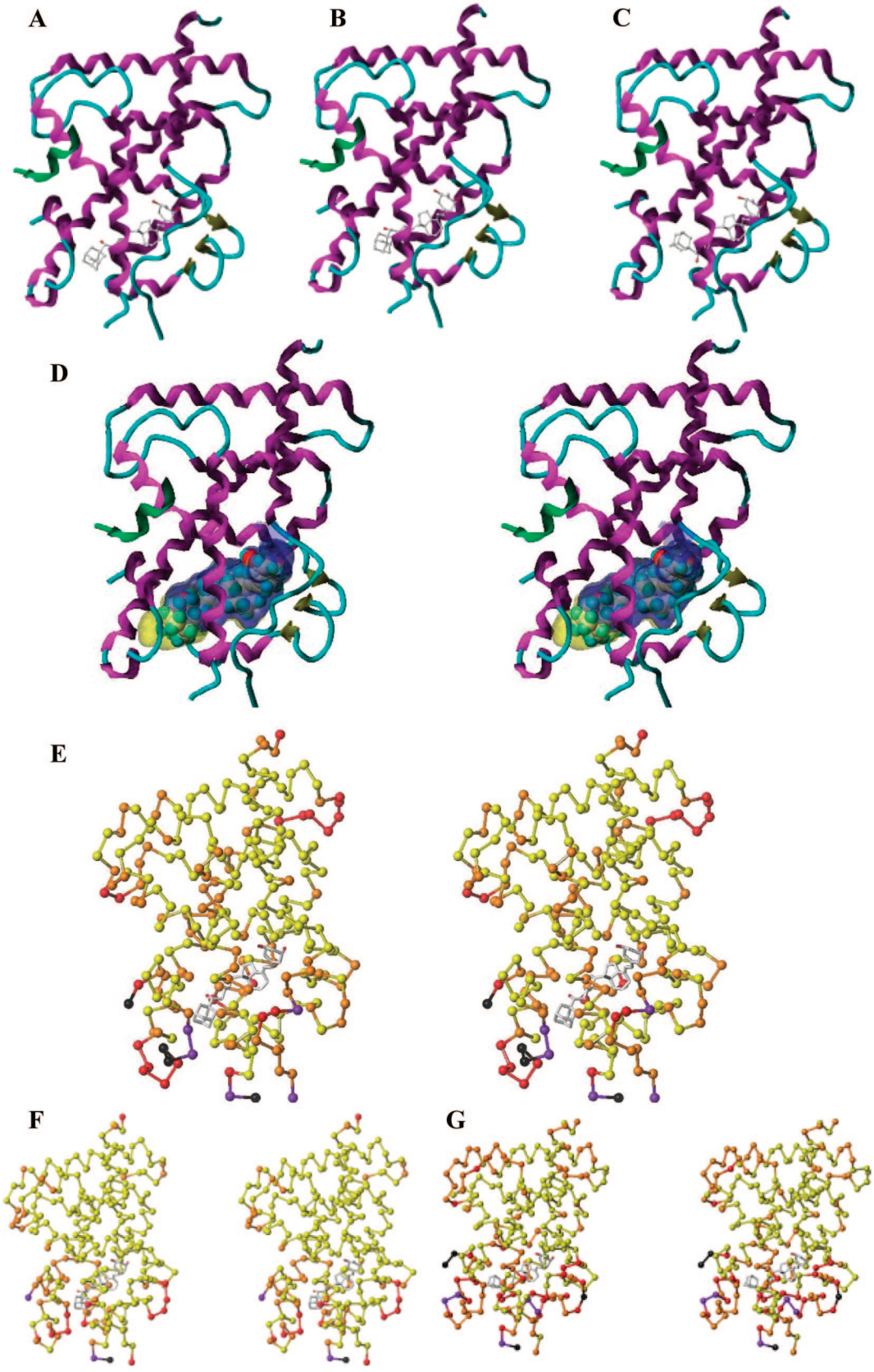


**Figure 2.** Crystal structures of the ternary complexes of the rVDR LBD (116−423, Δ165−211) with AD vitamin D compounds and a coactivator peptide derived from DRIP 205. The overall folds of the rVDR LBD bound to (A) **2a**, (B) **2b**, and (C) **2c** with ribbon-loop rendering and secondary-structure colors with the coactivator peptide in green and the ligands in stick representation with atom-type colors. (D) LBP of the rVDR LBD complexed with **2a** (transparent yellow) in comparison with that of the $1,25(OH)_2D_3$ complex (transparent blue) (stereoview, relaxed eyes). Individual Cα rms deviations of the rVDR complexes with (E) **2a**, (F) **2b**, and (G) **2c** shown on the LBD Cα structures. (≤0.24, 0.25−0.44, 0.45−0.74, 0.75−1.04, and ≥1.05 Å are yellow, orange, red, purple, and black, respectively.) (stereoview, relaxed eyes).

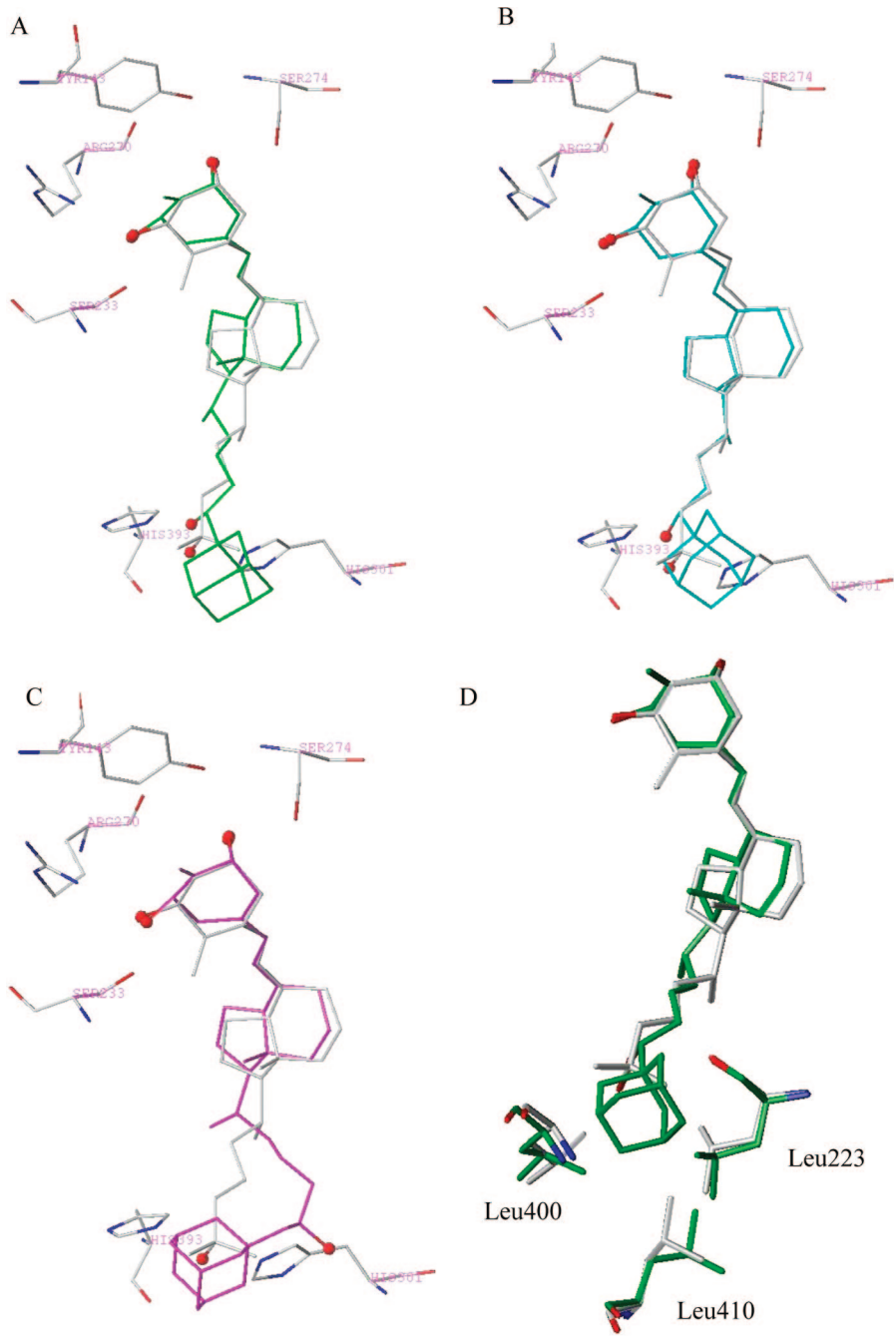


**Figure 3.** Overlay of ligands in the rVDR LBD complexes. The complexes were aligned at Cα atoms of the protein, and the ligands and some interacting residues are overlaid. (A) **2a** (green stick with red ball of oxygen), (B) **2b** (cyan stick with red ball of oxygen), and (C) **2c** (magenta stick with red ball of oxygen) are overlaid with **1** (atom-type stick with red ball of oxygen) accompanied by six residues that hydrogen bond with its three hydroxyl groups (shown in the same topology). (D) Ligand **2a** and three Leu residues (green stick with red oxygen) interacting with its AD moiety are overlaid with **1** and the same Leu residues (atom-type) in its complex.

LBP is not significantly changed when it binds superagonists with long, bulky side chains such as **3**[42] and **4** (Figure 1).[44]

**Complex with 2b.** The 24-adamantyl-24-hydroxyl compound **2b**, which has the shortest side chain of the three AD compounds, is a potential partial agonist of the VDR (VDR affinity is about 20% of that of **1**; transactivation, $EC_{50} = 2 \times 10^{-11}$ M; efficacy is 74% of that of **1**).[52] It forms three pairs of hydrogen bonds at its three hydroxyl groups (Figure 3B): 1α-OH, Ser233 and Arg270 (2.76 and 2.91 Å, respectively); 3β-OH, Tyr143 and Ser274 (2.96 and 3.00 Å, respectively); and 24-OH, His301 and His393 (2.93 and 2.55 Å, respectively). Compared with the $1,25(OH)_2D_3$ complex, significant Cα rms deviations are found in the residues that interact with the adamantane moiety and the 24-hydroxyl group, H3 N-terminal (Leu226∼Asp228), H6 to loop 6−7 (Val296∼Leu303), H11 (Glu391∼Lys395), and loop 11−12 (Leu400−Pro404 and Ser407−Thr411) (Figure 2F). Again, the rms deviations of the residues that form the AF-2 surface are minimal.

**Complex with 2c.** 26-Adamantyl-25-hydroxyl compound **2c** has the longest side chain of the three compounds and shows potent antagonistic activity (compared with **1**: VDR affinity, 1/20; transactivation, $EC_{50} = 2.4 \times 10^{-8}$ M; efficacy, 10%; antagonistic activity, $IC_{50} = 3 \times 10^{-8}$ M).[51] Compound **2c** is anchored in the LBP by two pairs of hydrogen bonds at the A-ring hydroxyl groups (Figure 3C): (1) 1α-OH, Ser233 and Arg270 (2.57 and 3.26 Å, respectively) and (2) 3β-OH, Tyr143

and Ser274 (2.67 and 2.90 Å, respectively). However, the side-chain hydroxyl group is not within hydrogen-bond distances from the two His residues (His301 and His393 (4.41 and 7.20 Å, respectively)). For this reason, **2c** has a lower VDR affinity than the other two compounds.

Because the 25-hydroxyl group is not fixed at H11 (His 393), the long and bulky side chain of **2c** could be packed in the LBP and could adopt a significantly different conformation compared with **2a** and **2b** (Figure 3A−C). Compared with those of the $1,25(OH)_2D_3$ complex, the Cα rms deviations are significant at a part of loop 1−3 that faces the 3β-hydroxyl group (Thr146−Asp152), at H6 to loop 6−7 (Tyr291−Leu303), and at the H11 N-terminal to loop 11−12 (Ser394−Leu410) (Figure 2G).

## Discussion

A number of crystal structures of NRs that are complexed with antagonists, partial agonists, or both have been reported.[23−30] Whereas NRs that are bound to agonist ligands invariably adopt the same canonical active conformation, those that are bound to antagonists/partial agonists exhibit various conformations. When ERα binds RAL[23] and OHT,[24] the bulky side chains with the tertiary amine group protrude from the LBP opening and are fixed on H3 (Asp351), forming a salt bridge via the amine group. In this way, the bulky ligands directly inhibit H12 from adopting the active conformation. Instead, H12 binds to the coactivator recognition surface (AF-2 surface) that mimicks the LXXLL motif of the coactivator NR box by its LLEML sequence. ERβ adopts a slightly different conformation when it binds the partial agonist genistein (GEN)[25] and the pure antagonist tetrahydrochrysene (THC) compound.[26] These ligands do not have a bulky substituent and are easily accommodated in the LBP. Therefore, these ligands do not directly interfere with H12, but H12 does not adopt the active conformation. It is placed over the LBP in a position such that it occludes the AF-2 surface only partially, and the transactivation is suppressed. This type of antagonism has been termed "passive antagonism" by Shiau et al.[26] as opposed to the active antagonism that was exhibited by RAL[23] and OHT.[24] The same ligands (GEN and THC) are similarly accommodated in the ERα, but here the H12 is in the active conformation, and the compounds act as agonists for ERα. It is reported that in the ERβ/THC complex, small differences (1.6−2.3 Å) in the positioning of residues on H11 cause this conformational and activity difference. So-called passive antagonists are rather common in other NRs such as progesterone and spironolactone for MR[27,28] and flutamide and bicalutamide for AR.[29,30] In the case of AR, it was possible to crystallize the complexes with antagonists only by mutating the residues that cause antagonism, and the mutant receptors were crystallized in the canonical active conformation. It was suggested that in the passive-type antagonist complexes the LBD body that accepts H12 is not properly folded so that H12 is not placed in the correct position for the active conformation. For the proper folding of the LBD body, the tight packing of H3 and H4/5 with the assistance of ligands and the correct positioning of H11 are believed to be important.[26−30]

We have investigated the structure−activity relationship of VDR ligands on the basis of their activity profiles in the 2D alanine scanning mutational analysis (2D ASMA) of all 34 VDR-LBP residues.[50] In this study, we also analyzed the behaviors of the two VDR antagonists/partial agonists, **7** and **8** (Figure 1),[50] compared with that of the full antagonist, **5**, and we classified these antagonists/partial agonists into two groups simply by whether they have bulky substituent (type I, **8** and **5**) or not (type II, **7**). Two groups of compounds showed distinct behaviors in the 2D ASMA.

The rVDR complexed with AD 19-norvitamin D compounds (**2a**−**c**), which show a series of partial agonistic (10−75% efficacy) to antagonistic activities, adopts the canonical active conformation; H12 is placed on the opening of the LBP, which forms the AF-2 surface to which the coactivator-peptide binds (Figure 2A−C). The bulky AD moiety does not crowd H12, as we proposed in our previous docking study,[50−53] but protrudes into the gap that is surrounded by the H11 C-terminus, loop 11−12, the H3 N-terminus, and loop 6−7. As a result, in all of these complexes, the LBPs are expanded (Figure 2D). These results contrast those that were obtained from VDR superagonists with long and bulky side chains, such as **3**[42] and **4** (Figure 1).[44] These superagonists reportedly do not widen the receptor LBP. Because of its bulkiness and rigidity, the AD side chain forces a change in the conformations of the VDR at N-terminal H3, loop 6−7, and H11 to loop 11−12, and weakens the interaction among these secondary structures. This structural change would destabilize the active conformation and reduce its contribution in the equilibrium among various conformations of the complexes (Figure 4).

Three AD 19-norvitamin D compounds (**2a**−**2c**) can be categorized as type I antagonists by our definition, but they are difficult to classify as either active- or passive-type antagonists.

The schematic molecular mechanism in Figure 4 explains the activity profiles of the AD 19-norvitamin D series. The VDR LBD complexed with AD vitamin D ligands (**2a**−**2c**) adopts multiple relatively stabilized conformations (**D**, **E**, **F**, etc.). Whether the ligand exhibits agonist or antagonistic activity depends on the population of these conformations and the concentrations of coactivator (**CoA**) and corepressor (**CoR**) complexes under given cellular conditions. The population of the active conformation (**F**) would decrease in the order **2b** > **2a** ≫ **2c**; accordingly, the transcriptional activities would decrease in the same order. However, the transcriptional activities of these compounds (**2a**−**2c**) would be changed in a cell and tissue context-dependent manner following the equilibrium shown in Figure 4. If the **CoA** complex level is high, then the equilibrium between complexes **F** and **H** shifts to **H**, and agonistic activities would become predominant. If the **CoA** complex level is low, the **CoR** complex level is high, or both, then the whole equilibrium among complexes **D** to **H** would converge to **G**, and transactivation would be suppressed.[15] Complexes of coactivators and corepressors possess sensing activities for multiple signaling pathways[16] and thus the activities of VDR ligands are affected by cell signaling via the regulation of these coregulator levels.

## Conclusions

The crystal structures of the rVDR LBD complexed with a series of AD 19-norvitamin D compounds (**2a**−**2c**) and a coactivator peptide derived from DRIP205 have been solved. These complexes adopt the canonical active conformation, and the coactivator peptide binds to the AF-2 surface, regardless of the partial agonistic/antagonistic activities of the ligands. We suggest that the rigid and bulky adamantyl side chain that protrudes into a gap formed by the H11 C-terminus, loop 11−12, the H3 N-terminus, and loop 6−7 weakens the interactions among these secondary structures and destabilizes the active conformation. As a result, the contribution of the active conformation in the equilibrium among multiple protein conformations is significantly reduced, and the transcriptional potencies of these compounds (**2a**−**2c**) are decreased. The

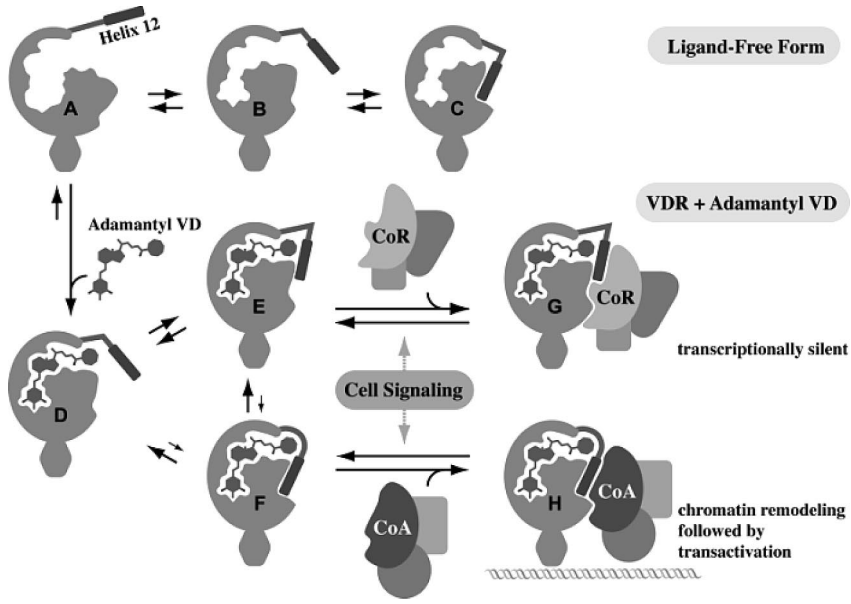


**Figure 4.** Molecular mechanism of the transactivation regulated by the VDR.

results presented a structural basis for VDR antagonism and partial agonism for the first time.

## Experimental Section

**General.** All nonaqueous reactions were carried out under argon or nitrogen in freshly distilled anhydrous solvents. In all chemical reactions, the products underwent a general workup procedure that included extraction with organic solvents, solvent evaporation after drying the extracts over anhydrous $MgSO_4$, and purification by column chromatography on silica gel. We conducted high-pressure liquid chromatography (HPLC) by using Jasco 880-PU pumps equipped with an 801-SC solvent programmer and a Uvidec-100V variable-length UV−vis detector. Nuclear magnetic resonance ($^1H$ and $^{13}C$) spectra were recorded in $CDCl_3$ solution on a Bruker ARX 400 MHz spectrometer. Low- (MS) and high-resolution mass spectra (HRMS) were obtained by electronic ionization (70 eV) on a JEOL JMS-AX505HA spectrometer. Ultraviolet spectra were recorded on a Hitachi U-3200 spectrophotometer.

**Chemicals.** 26-Adamantyl-1α,25*R*-dihydroxy-2-methylene-22,23-didehydro-19,27-dinor-20-epivitamin $D_3$ (**2c**) was synthesized in our laboratory as reported.[51] All commercial reagents were used without further purification.

**3-Adamantan-1-yl-3-hydroxy-propionic Acid Ethyl Ester (4a).** To a refluxing suspension of aldehyde **3** (1.11 g, 6.75 mmol) and Zn powder (573 mg, 8.75 mmol) in benzene (13 mL) was added ethyl bromoacetate (895 μL, 8.10 mmol) in one portion, and the mixture was refluxed for 40 min. After the reaction was cooled to 0 °C, 3% HCl was added to the reaction, and the whole mixture was extracted with $CH_2Cl_2$. After a general workup, ethyl ester **4a** (1.24 g, 72.9%) was obtained as a colorless oil. $^1H$ NMR (**4a**, δ): 1.28 (3H, t, $J$ = 7.2 Hz), 1.4−1.8 (12H, m), 2.0 (3H, m), 2.36 (1H, dd, $J$ = 16.1 and 10.5 Hz), 2.52 (1H, dd, $J$ = 16.1 and 2.3 Hz), 2.74 (1H, d, $J$ = 3.8 Hz), 3.54 (1H, m), 4.17 (2H, q, $J$ = 7.2 Hz).

**3-Adamantan-1-yl-3-triethylsilanyloxy-propionic Acid Ethyl Ester (4b).** Imidazole (3.4 g, 50 mmol) and $Et_3SiCl$ (4.2 mL, 25.0 mmol) were added to a solution of **4a** (2.10 g, 8.32 mmol) in DMF (20 mL), and the mixture was stirred at room temperature for 3 h. The reaction was cooled (0 °C), quenched with water, and worked up to yield triethylsilyl ether **4b** (2.87 g, 94.2%). $^1H$ NMR (**4b**, δ): 0.60 (6H, q, $J$ = 7.9 Hz), 0.95 (9H, t, $J$ = 7.9 Hz), 1.27 (3H, t, $J$ = 7.2 Hz), 1.4−1.8 (12H, m), 1.97 (3H, m), 2.29 (1H, dd, $J$ = 15.8 and 7.8 Hz), 2.56 (1H, dd, $J$ = 15.8 and 3.8 Hz), 3.74 (1H, dd, $J$ = 7.8 Hz), 4.14 (2H, m).

**(1-Adamantan-1-yl-3-benzenesulfonyl-propoxy)-triethylsilane (5d).** A toluene solution of DIBAL-H (1.02 M, 12.8 mL, 13.1 mmol) was added to a solution of **4b** (1.6 g, 4.37 mmol) in toluene (10 mL) at −78 °C, and the mixture was stirred for 1.5 h at the same temperature. The reaction was quenched with 10% potassium sodium tartrate solution and was then worked up to yield alcohol derivative **5a** (1.4 g, 98.3%). This alcohol was dissolved in dry pyridine (6 mL). TsCl (1.43 mL, 7.5 mmol) was added to this solution at 0 °C, and the whole solution was stirred for 4 h at that temperature. The reaction was quenched with water at 0 °C for 1 h and was worked up to yield tosylate **5b** (1.87 g, 91%). Thiophenol (445 mL, 4.33 mmol) and t-BuOK (526.8 mg, 4.69 mmol) were added to a solution of **5b** (1.73 g, 3.61 mmol) in DMF (16 mL), and the mixture was stirred at 0 °C for 40 min. The reaction was quenched with water and was then worked up to yield sulfide **5c** (1.24 g, 83%). M-CPBA (65%, 1.82 mg, 6.89 mmol) was added to a solution of sulfide **5c** (1.31 g, 3.13 mmol) in $CH_2Cl_2$ (26 mL) at 0 °C, and the mixture was stirred for 30 min at 0 °C and for 2 h at room temperature. Water was added to the reaction, and the mixture was worked up to produce sulfone **5d** (1.32 g, 94%). $^1H$ NMR (**5d**, δ): 0.536, 0.541 (6H, q, $J$ = 7.9 Hz), 0.91 (9H, t, $J$ = 7.9 Hz), 1.3−1.8 (12H, m), 1.95 (3H, m), 3.05 (1H, m), 3.16 (1H, dd, $J$ = 7.6 and 3.5 Hz), 3.25 (1H, m), 7.58 (2H, m), 7.67 (1H, m), 7.91 (2H, m).

**25-Adamantyl-1α,25-dihydroxy-2-methylene-22,23-didehydro-19,26,27-trinor-20-epivitamin $D_3$ 1,3-Bis-(tert-butyl-trimethysilyl) 25-triethylsilyl Ether (11).** Diisopropylamine (28 μL, 0.2 mmol), followed by *n*-BuLi (1.54 M hexane solution, 107 μL, 0.16 mmol), was added to a solution of sulfone **5d** (74 mg, 0.17 mmol) in THF (500 μL) at −20 °C, and the mixture was stirred for 10 min at that temperature. To this mixture, a solution of aldehyde **8**[51] (62.8 mg, 0.11 mmol) in THF (750 μL) was added, and the reaction continued to be stirred at −20 °C for 20 min. The reaction was quenched with water and was worked up to yield **9** (146 mg) as a mixture of diastereomers. Hydroxyl sulfone **9** (124 mg) was dissolved in pyridine (1 mL) and was treated with acetic anhydride (115 μL, 1.22 mmol) and dimethylaminopyridine (3.2 mg, 0.026 mmol) at room temperature for 4 h. Acetate **10** (123 mg) was obtained after a general workup. Na−Hg (10%, 403 mg, 1.8 mmol) and $Na_2HPO_4$ (254 mg, 1.8 mmol) were added to a solution of acetate **10** in THF (1 mL) at 0 °C, and then the mixture was stirred at room temperature for 1 h. The reaction was quenched with 1 N HCl and was worked up to yield bis-TBS ether **11** as a 1:1 mixture of C25 epimers (38.1 mg, 37.4% from **8**). $^1H$ NMR (**11**, δ): 0.03, 0.05, 0.07, 0.08 (each 3H, s), 0.51 (3H, s), 0.61 (6H, m), 0.86, 0.89 (each 9H, s), 0.95

(9H, m), 2.81 (1H, m), 3.13 (1H, m), 4.42 (2H, m), 4.92 (1H, s), 4.97 (1H, s), 5.2−5.5 (2H, m), 5.83 (1H, d, $J$ = 11.3 Hz), 6.21 (1H, d, $J$ = 11.3 Hz).

**(25*R*)-25-Adamantyl-1α,25-dihydroxy-2-methylene-22,23-didehydro-19,26,27-trinor-20-epivitamin $D_3$ (2a).** Camphor sulfonic acid (50.1 mg, 0.22 mmol) was added to a solution of silyl ether **11** (46.4 mg, 0.054 mmol) in MeOH (1 mL) at room temperature, and the mixture was stirred for 2.5 h. The reaction was quenched with 5% $NaHCO_3$ and was worked up to yield a 1:1 mixture of **2a** and its C25 epimer **2a′** (22.5 mg, 80.5%), which were separated by HPLC (YMC-Pack ODS-AM SH-342-5; 150 × 20 $mm^2$; $H_2O$/MeOH, 1/9; 8 mL/min) to give **2a** (11 mg) and **2a′** (10.5 mg), which eluted in this order. $^1$H NMR (**2a** (25*R* epimer), δ): 0.52 (3H, s), 0.94 (3H, d, $J$ = 6.6 Hz), 3.01 (1H, dd, $J$ = 10.7 and 1.8 Hz), 4.49 (2H, m), 5.09 (1H, s), 5.11 (1H, s), 5.33 (1H, ddd, $J$ = 15.2, 8.6, and 5.0 Hz), 5.44 (1H, dd, $J$ = 15.2 and 9.2 Hz), 5.88 (1H, d, $J$ = 11.0 Hz), 6.36 (1H, d, $J$ = 11.0 Hz). MS *m*/*z* (%): 520 ($M^+$, 28), 520 (20), 484 (10), 251 (35), 223 (15), 165 (60), 135 (100), 105 (45). HRMS: calcd for $C_{35}H_{52}O_3$, 520.3916; found, 520.3925. UV (95% EtOH) $\lambda_{max}$, nm (log ε): 246 (4.48), 254 (4.54), 263 (4.37). $^1$H NMR (**2a′** (25*S* epimer), δ): 0.53 (3H, s), 0.93 (3H, d, $J$ = 6.6 Hz), 3.07 (1H, m), 4.49 (2H, m), 5.09 (1H, s), 5.11 (1H, s), 5.41 (2H, m), 5.87 (1H, d, $J$ = 11.0 Hz), 6.35 (1H, d, $J$ = 11.0 Hz). MS *m*/*z* (%): 520 ($M^+$, 8), 385 (65), 251 (10), 165 (30), 133 (100), 79 (25). HRMS: calcd for $C_{35}H_{52}O_3$, 520.3916; found, 520.3918. UV (95% EtOH) $\lambda_{max}$, nm: 246, 254, 263.

**Adamantan-1-yl-trimethylsilanyloxy-acetonitrile (6).** TMSCN (346 μL, 2.6 mmol) and $ZnI_2$ (24.6 mg, 0.077 mmol) were added to a solution of aldehyde **3** (213 mg, 1.3 mmol) in $CH_2Cl_2$ (5 mL) at 0 °C, and the mixture was stirred for 1 h at that temperature. The reaction was quenched with 5% $Na_2S_2O_3$ solution at 0 °C and was then worked up to produce cyanide **6** (257 mg, 75.3%). $^1$H NMR (**6**, δ): 0.19 (9H, s), 1.5−1.8 (12H, m), 1.9−2.2 (3H, m), 3.86 (1H, s). $^{13}$C NMR (**6**, δ): −0.3, 28.1, 36.9, 37.3, 37.6, 71.3, 119.0. MS *m*/*z* (%): 263 ($M^+$, 8), 248 (10), 135 (100), 107 (5), 93 (8), 79 (89, 73 (5).

**Adamantan-1-yl-trimethylsilanyloxy-acetaldehyde (7).** A toluene solution of DIBAL-H (1.01 M, 135 μL, 0.14 mmol) was added to a solution of cyanide **6** (24 mg, 0.091 mmol) in $CH_2Cl_2$ (500 μL) at 0 °C, and the mixture was stirred for 1 h at that temperature. The reaction was quenched with 10% potassium sodium tartrate solution and was worked up to yield aldehyde **7** (166 mg, 68.7%). $^1$H NMR (**7**, δ): 0.10 (9H, s), 1.5−1.8 (12H, m), 1.9−2.2 (3H, m), 3.33 (1H, d, $J$ = 2.9 Hz), 9.65 (1H, d, $J$ = 2.9 Hz). $^{13}$C NMR (**7**, δ): 0.2, 28.4, 37.1, 38.0, 38.3, 85.0, 205.6. MS *m*/*z* (%): 237 ($M^+$ − $C_2H_5$, 87), 135 (100), 107 (5), 93 (12), 73 (42).

**1α-Hydroxy-2-methylene-22-phenylsulfanyl-19,23,24,25,26,27-hexanorvitamin $D_3$ 1,3-Bis-(tert-butyl-dimethylsilyl) Ether (13a).** Tosylate **12** was treated with thiophenol under conditions similar to those described in the synthesis of **5c** to produce **13a** (99.8%). $^1$H NMR (**13a**, δ): 0.02, 0.05, 0.06, 0.08 (each 3H, s), 0.54 (3H, s), 0.86, 0.89 (each 9H, s), 1.13 (3H, d, $J$ = 6.5 Hz), 2.68 (1H, dd, $J$ = 12.1 and 8.8 Hz), 2.82 (1H, m), 3.15 (1H, dd, $J$ = 12.1 and 2.7 Hz), 4.42 (2H, m), 4.92 (1H, s), 4.97 (1H, s), 5.84 (1H, d, $J$ = 11.2 Hz), 6.21 (1H, d, $J$ = 11.2 Hz), 7.15 (1H, m), 7.26 (2H, m), 7.33 (2H, m). $^{13}$C NMR (**13a**, δ): −4.9, −4.7, −4.6, 12.3, 18.4, 18.5, 19.2, 22.4, 23.6, 26.0, 26.1, 27.8, 28.9, 37.0, 38.8, 40.6, 41.4, 46.1, 47.8, 56.0, 56.3, 71.9, 72.7, 106.5, 116.5, 122.5, 125.7, 129.0, 129.1, 133.2, 138.0, 141.0, 153.1. IR (neat, $cm^{-1}$): 2927, 2855, 1253, 1101, 836. MS *m*/*z* (%): 666 ($M^+$, 18), 609 (10), 534 (100), 477 (5), 402 (20), 366 (25), 309 (5), 279 (8), 251 (10), 197 (12), 147 (10), 123 (12), 75 (55), 73 (40).

**1α-Hydroxy-2-methylene-22-phenylsulfonyl-19,23,24,25,26,27-hexanorvitamin $D_3$ 1,3-Bis-(tert-butyl-dimethylsilyl) Ether (13b).** To a solution of **13a** (19 mg, 0.028 mmol) in $CH_2Cl_2$/MeOH (3/5, 800 μL) was added sodium tungstate(VI) dihydrate (14.7 mg, 0.045 mmol) at 0 °C. After 5 min, 30% $H_2O_2$ (50 μL) was added, and the whole mixture was stirred for 7.5 h at room temperature. The reaction was quenched with 2 N $Na_2S_2O_3$ at 0 °C, and it underwent a general workup to produce sulfone **13b** (12.8 mg, 65%) and the corresponding sulfoxide (5.1 mg, 26.3%). $^1$H NMR (**13b**, δ): 0.02, 0.04, 0.06, 0.07 (each 3H, s), 0.52 (3H, s), 0.86, 0.89 (each 9H, s), 1.20 (3H, d, $J$ = 6.5 Hz), 2.79 (1H, m), 2.87 (1H, dd, $J$ = 14.2 and 9.6 Hz), 3.16 (1H, m), 4.41 (2H, m), 4.92 (1H, s), 4.97 (1H, s), 5.80 (1H, d, $J$ = 11.2 Hz), 6.19 (1H, d, $J$ = 11.2 Hz), 7.57 (2H, m), 7.63 (1H, m), 7.91 (2H, m). $^{13}$C NMR (**13b**, δ): −4.9, −4.7, 12.1, 18.4, 18.5, 20.5, 22.3, 23.4, 26.0, 26.3, 27.7, 28.8, 32.8, 38.8, 40.5, 45.9, 47.8, 56.0, 56.4, 62.3, 71.8, 72.7, 106.6, 116.8, 122.4, 128.1, 129.5, 133.5, 133.7, 140.4, 140.6, 153.1. IR (neat, $cm^{-1}$): 2952, 2928, 2855, 1471, 1306, 1252, 1147, 1086. MS *m*/*z* (%): 698 ($M^+$, 15), 683 (3), 641 (18), 566 (100), 509 (30), 424 (10), 366 (35), 351 (5), 293 (8), 257 (10), 197 (8), 147 (12), 135 (10), 73 (60). HRMS: calcd for $C_{40}H_{66}O_4Si_2S$, 698.4220; found, 698.4235.

**24-Adamantyl-1α,24-dihydroxy-2-methylene-22,23-didehydro-19,25,26,27-tetranorvitamin $D_3$ 1,3-Bis-(tert-butyl-dimethylsilyl) Ether (17a and 17b).** To a solution of sulfone **13b** (34.2 mg, 0.049 mmol) in THF (500 μL) at −20 °C was added diisopropylamine (21 μL, 0.15 mmol), followed by *n*-BuLi (1.54 M hexane solution, 80 μL, 0.12 mmol), and the resulting yellow solution was stirred for 10 min at that temperature. To this solution was added a solution of aldehyde **7** (25.4 mg, 0.096 mmol) in THF (500 μL), and the mixture was stirred for 30 min at the same temperature. The reaction was quenched with water, and it then underwent a general workup procedure to yield a complex mixture of diastereomers of coupling product **14** (49 mg). The TMS ether was deprotected by treating **14** (49 mg) with AcOH/THF/$H_2O$ (8/8/1, 1 mL) at room temperature for 20 h. A 5% $NaHCO_3$ solution was added to the reaction at 0 °C, and the mixture was worked up to yield **15** (29.5 mg). Diol **15** was acetylated by treatment with $Ac_2O$ (150 μL) and DMAP (3.9 mg, 0.032 mmol) in pyridine (500 μL) at room temperature for 6 h. The reaction was quenched with water at 0 °C for 1 h and was then worked up to produce acetate **16** (29.5 mg). This acetate was dissolved in THF (400 mL) and MeOH (600 mL), was cooled to 0 °C, was treated with $Na_2HPO_4$ (190 mg, 1.3 mmol) and 10% Na−Hg (306 mg, 1.3 mmol), and was then stirred at room temperature for 3 h. The reaction was quenched with 10% HCl at 0 °C and was worked up to produce less-polar **17a** (4.6 mg, 17.4% from **12**) and more-polar **17b** (4.4 mg, 16.6% from **12**). $^1$H NMR (**17a**, δ): 0.03, 0.05, 0.07, 0.08 (each 3H, s), 0.57 (3H, s), 0.86, 0.89 (each 9H, s), 1.05 (3H, d, $J$ = 6.6 Hz), 2.83 (1H, m), 3.47 (1H, m), 4.42 (2H, m), 4.92 (1H, s), 4.97 (1H, s), 5.45 (2H, m), 5.83 (1H, d, $J$ = 11.2 Hz), 6.22 (1H, d, $J$ = 11.2 Hz). IR (neat, $cm^{-1}$): 3749, 2927, 1716, 1540, 1507. MS *m*/*z* (%): 716 ($M^+$ − $H_2O$, 22), 659 (3), 602 (50), 584 (70), 513 (5), 467 (7), 449 (6), 366 (45), 351 (8), 234 (10), 135 (100), 73 (50). HRMS: calcd for $C_{46}H_{78}O_3Si_2$, 734.5489; found, 734.5468. $^1$H NMR (**17b**, δ): 0.02, 0.05, 0.06, 0.08 (each 3H, s), 0.57 (3H, s), 0.86, 0.89 (each 9H, s), 1.05 (3H, d, $J$ = 6.5 Hz), 2.83 (1H, m), 3.49 (1H, m), 4.43 (2H, m), 4.92 (1H, s), 4.97 (1H, s), 5.47 (2H, m), 5.84 (1H, d, $J$ = 11.1 Hz), 6.22 (1H, d, $J$ = 11.1 Hz). IR (neat, $cm^{-1}$): 3749, 2927, 2902, 2853, 1732, 1541, 1256. MS *m*/*z* (%): 716 ($M^+$ − $H_2O$, 10), 659 (2), 602 (38), 584 (36), 513 (2), 467 (5), 449 (3), 366 (32), 351 (5), 234 (10), 197 (12), 135 (100), 93 (15), 73 (65).

**(24*R*)-24-Adamantyl-1α,24-dihydroxy-2-methylene-22,23-didehydro-19,25,26,27-tetranorvitamin $D_3$ (2b).** A solution of *n*-$Bu_4NF$ (1 M THF solution, 48 μL, 0.048 mmol) was added to a solution of **17a** (3.5 mg, 4.8 μmol) in THF (200 μL) at room temperature, and the mixture was stirred for 6.5 h. The reaction was quenched with water and was then worked up to yield **2b** (2.4 mg, 98.8%). $^1$H NMR (**2b**, δ): 0.58 (3H, s), 1.06 (3H, d, $J$ = 6.6 Hz), 3.48 (1H, m), 4.47 (2H, m), 5.09 (1H, s), 5.11 (1H, s), 5.45 (2H, m), 5.89 (1H, d, $J$ = 11.2 Hz), 6.36 (1H, d, $J$ = 11.2 Hz). MS *m*/*z* (%): 506 ($M^+$, 15), 452 (20), 437 (5), 251 (12), 202 (10), 135 (100), 93 (20), 79 (18). HRMS: calcd for $C_{34}H_{50}O_3$, 506.3760; found, 506.3755. UV (95% EtOH) $\lambda_{max}$, nm: 245, 254, 263.

**Protein Expression and Purification.** The rat VDR LBD (residues 116−423, Δ165−211) was cloned as an N-terminal $His_6$-tagged fusion protein into the pET14b expression vector and was overproduced in *Escherichia coli* C41. The cells were grown at 37 °C in LB medium (including 100 mg/L ampicilin) and were subsequently induced for 6 h with 15 μM isopropyl-β-D-thiogalactopyranoside (IPTG) at 23 °C. The purification procedure included

affinity chromatography on a Ni-NTA column, followed by dialysis and ion-exchange chromatography (SP-Sepharose). After tag removal by thrombin digestion, the protease was removed by filtration through a HiTrap benzamidine column, and the protein was further purified by gel filtration on a Superdex200 column. The purity and homogeneity of the rVDR LBP were assessed by SDS-PAGE.

**Crystallization.** Purified rVDR LBD solution was concentrated to about 0.75 mg/mL by ultrafiltration. To an aliquot (800 $\mu$L) of the protein solution was added a ligand (ca. 10 equiv); the solution was further concentrated to about 1/8, and then a solution (25 mM Tris-HCl, pH 8.0; 50 mM NaCl; 10 mM DTT; 0.02% $NaN_3$) of coactivator peptide ($H_2N$-KNHPMLMNLLKDN-$CONH_2$) derived from DRIP205 was added. This solution of VDR/ligand/peptide was allowed to crystallize by the vapor-diffusion method that used a series of precipitant solutions containing 0.1 M MOPS-NaOH (pH 7.0), 0.1−0.4 M sodium formate, 12−22% (w/v) PEG4000, and 5% (v/v) ethylene glycol. Droplets for crystallization were prepared by mixing 2 $\mu$L of complex solution and 1 $\mu$L of precipitant solution, and droplets were equilibrated against 500 $\mu$L of precipitant solution at 20 °C. It took 1 to 2 days to obtain crystals of X-ray diffraction quality for VDR complexes with $1,25(OH)_2D_3$, **2a**, or **2b** as a ligand.

**Diffraction Experiment and Structure Analysis.** Prior to the diffraction data collection, crystals were soaked in a cryoprotectant solution that contained 0.1 M MOPS-NaOH (pH 7.0), 0.1−0.4 M sodium formate, 15−20% PEG4000, and 17−20% ethylene glycol. Diffraction data sets were collected at 100 K in a stream of nitrogen gas at beamlines BL-6A of KEK-PF and NW12A of PF-AR (Tsukuba, Japan). Reflections were recorded with an oscillation range per image of 1.0°. Diffraction data were indexed, integrated, and scaled using the program HKL2000.[56] The structures of the complex were solved by molecular replacement with the program CNS,[57] and finalized sets of atomic coordinates were obtained after iterative rounds of model modification with the program XtalView[58] and after refinement with CNS by rigid body refinement, simulated annealing, positional minimization, water molecule identification, and individual isotropic *B*-value refinement. We calculated the LBP volumes of the VDR/adamantyl vitamin D and $1,25(OH)_2D_3$ complexes by using the fast Connolly channel surface program of the SYBYL molecular modeling software (Tripos, St. Louis).

**Supporting Information Available:** Data collection and refinement statistics of rVDR complexes. This material is available free of charge via the Internet at http://pubs.acs.org.

## References


(1) Yamada, S.; Shimizu, M.; Yamamoto, K. Vitamin D Receptor. In *Vitamin D and Rickets*; Hochberg, Z., Ed.; Karger: New York, 2003; pp 50−68.

(2) McDonnell, D. P.; Mangelsdorf, D. J.; Pike, J. W.; Haussler, M. R.; O'Malley, B. W. Molecular cloning of complementary DNA encoding the avian receptor for vitamin D. *Science* **1987**, *235*, 1214–1217.

(3) Baker, A. R.; McDonnell, D. P.; Hughes, M. R.; Crisp, T. M.; Mangelsdorf, D. J.; Haussler, M. R.; Pike, J. W.; Shine, J. Cloning and expression of full-length cDNA encoding human vitamin D receptor. *Proc. Natl. Acad. Sci. U.S.A.* **1988**, *85*, 3294–3298.

(4) Burmester, J. K.; Maeda, N.; DeLuca, H. F. Isolation and expression of rat 1,25-dihydroxyvitamin D receptor cDNA. *Proc. Natl. Acad. Sci. U.S.A.* **1988**, *85*, 1005–1009.

(5) Kamei, Y.; Kawada, T.; Fukuwatari, T.; Ono, T.; Kato, S.; Sugimoto, E. Cloning and sequencing of the gene encoding the mouse vitamin D receptor. *Gene* **1995**, *152*, 281–282.

(6) Li, Y. C.; Bergwitz, C.; Juppner, H.; Demay, M. B. Cloning and characterization of the vitamin D receptor from *Xenopus laevis*. *Endocrinology* **1997**, *138*, 2347–2353.

(7) Chun, R. F.; Chen, H.; Boldrick, L.; Sweet, C.; Adams, J. S. Cloning, sequencing, and functional characterization of the vitamin D receptor in vitamin D-resistant New World primates. *Am. J. Primatol.* **2001**, *54*, 107–118.

(8) Mangelsdorf, D. J.; Thummel, C.; Beato, M.; Herrlich, P.; Schutz, G.; Umesono, K.; Blumberg, B.; Kastner, P.; Mark, M.; Chambon, P.; Evans, R. M. The nuclear receptor superfamily: the second decade. *Cell* **1995**, *83*, 835–839.

(9) Tsai, M. J.; O'Malley, B. W. Molecular mechanisms of action of steroid/thyroid receptor superfamily members. *Annu. Rev. Biochem.* **1994**, *63*, 451486.

(10) DeLuca, H. F. Overview of general physiologic features and functions of vitamin D. *Am. J. Clin. Nutr.* **2004**, *80*, 1689S–1696S.

(11) Emerging Therapeutic Uses. In *Vitamin D*; Feldman, D., Glorieux, F. H., Pike, J. W., Eds.; Academic Press: New York, 1997, pp 1089−1227.

(12) Yamada, S.; Shimizu, M.; Yamamoto, K. Structure-function relationships of vitamin D including ligand recognition by the vitamin D receptor. *Med. Res. Rev.* **2003**, *23*, 89–115.

(13) Yamada, S.; Yamamoto, K. Ligand recognition by vitamin D receptor: total alanine scanning mutational analysis of the residues lining the ligand binding pocket of vitamin D receptor. *Curr. Top. Med. Chem.* **2006**, *6*, 1255–1265.

(14) Makishima, M.; Yamada, S. Targeting the vitamin D receptor: advances in drug discovery. *Expert Opin. Ther. Pat.* **2005**, *15*, 1133–1145.

(15) Smith, C. L.; O'Malley, B. W. Coregulator function: a key to understanding tissue specificity of selective receptor modulators. *Endocr. Rev.* **2004**, *25*, 45–71.

(16) Rosenfeld, M. G.; Lunyak, V. V.; Glass, C. K. Sensors and signals: a coactivator/corepressor/epigenetic code for integrating signal-dependent programs of transcriptional response. *Genes Dev.* **2006**, *20*, 1405–1428.

(17) Aoyagi, S.; Archer, T. K. Dynamics of coactivator recruitment and chromatin modifications during nuclear receptor mediated transcription. *Mol. Cell. Endocrinol.* **2008**, *280*, 1–5.

(18) Jordan, V. C. The strategic use of antiestrogens to control the development and growth of breast cancer. *Cancer* **1992**, *70*, 977–982.

(19) Delmas, P. D.; Bjarnason, N. H.; Mitlak, B. H.; Ravoux, A. C.; Shah, A. S.; Huster, W. J.; Draper, M.; Christiansen, C. Effects of raloxifene on bone mineral density, serum cholesterol concentrations, and uterine endometrium in postmenopausal women. *N. Engl. J. Med.* **1997**, *337*, 1641–1647.

(20) Sutanto, W.; de Kloet, E. R. Mineralocorticoid receptor ligands: biochemical, pharmacological, and clinical aspects. *Med. Res. Rev.* **1991**, *11*, 617–639.

(21) Kolvenbag, G. J.; Furr, B. J. Relative potency of bicalutamide (casodex) and flutamide (eulexin). *Urology* **1999**, *54*, 194–197.

(22) Fradet, Y. Bicalutamide (casodex) in the treatment of prostate cancer. *Expert Rev. Anticancer Ther.* **2004**, *4*, 37–48.

(23) Brzozowski, A. M.; Pike, A. C.; Dauter, Z.; Hubbard, R. E.; Bonn, T.; Engstrom, O.; Ohman, L.; Greene, G. L.; Gustafsson, J. A.; Carlquist, M. Molecular basis of agonism and antagonism in the oestrogen receptor. *Nature* **1997**, *389*, 753–758.

(24) Shiau, A. K.; Barstad, D.; Loria, P. M.; Cheng, L.; Kushner, P. J.; Agard, D. A.; Greene, G. L. The structural basis of estrogen receptor/coactivator recognition and the antagonism of this interaction by tamoxifen. *Cell* **1998**, *95*, 927–937.

(25) Pike, A. C.; Brzozowski, A. M.; Hubbard, R. E.; Bonn, T.; Thorsell, A. G.; Engström, O.; Ljunggren, J.; Gustafsson, J. A.; Carlquist, M. Structure of the ligand-binding domain of oestrogen receptor beta in the presence of a partial agonist and a full antagonist. *EMBO J.* **1999**, *18*, 4608–4618.

(26) Shiau, A. K.; Barstad, D.; Radek, J. T.; Meyers, M. J.; Nettles, K. W.; Katzenellenbogen, B. S.; Katzenellenbogen, J. A.; Agard, D. A.; Greene, G. L. Structural characterization of a subtype-selective ligand reveals a novel mode of estrogen receptor antagonism. *Nat. Struct. Biol.* **2002**, *9*, 359–364.

(27) Bledsoe, R. K.; Madauss, K. P.; Holt, J. A.; Apolito, C. J.; Lambert, M. H.; Pearce, K. H.; Stanley, T. B.; Stewart, E. L.; Trump, R. P.; Willson, T. M.; Williams, S. P. A ligand-mediated hydrogen bond network required for the activation of the mineralocorticoid receptor. *J. Biol. Chem.* **2005**, *280*, 31283–31293.

(28) Fagart, J.; Huyet, J.; Pinon, G. M.; Rochel, M.; Mayer, C.; Rafestin-Oblin, M. E. Crystal structure of a mutant mineralocorticoid receptor responsible for hypertension. *Nat. Struct. Mol. Biol.* **2005**, *12*, 554–555.

(29) Bohl, C. E.; Gao, W.; Miller, D. D.; Bell, C. E.; Dalton, J. T. Structural basis for antagonism and resistance of bicalutamide in prostate cancer. *Proc. Natl. Acad. Sci. U.S.A.* **2005**, *102*, 6201–6206.

(30) Bohl, C. E.; Miller, D. D.; Chen, J.; Bell, C. E.; Dalton, J. T. Structural basis for accommodation of nonsteroidal ligands in the androgen receptor. *J. Biol. Chem.* **2005**, *280*, 37747–37754.

(31) Bury, Y.; Steinmeyer, A.; Carlberg, C. Structure activity relationship of carboxylic ester antagonists of the vitamin $D_3$ receptor. *Mol. Pharmacol.* **2000**, *58*, 1067–1074.

(32) Väisänen, S.; Peräkylä, M.; Kärkkäinen, J. I.; Steinmeyer, A.; Carlberg, C. Critical role of helix 12 of the vitamin $D_3$ receptor for the partial agonism of carboxylic ester antagonists. *J. Mol. Biol.* **2002**, *315*, 229–238.

(33) Lempiäinen, H.; Molnár, F.; Macias Gonzalez, M.; Peräkylä, M.; Carlberg, C. Antagonist- and inverse agonist-driven interactions of the vitamin D receptor and the constitutive androstane receptor with corepressor protein. *Mol. Endocrinol.* **2005**, *19*, 2258–2272.

(34) Toell, A.; Gonzalez, M. M.; Ruf, D.; Steinmeyer, A.; Ishizuka, S.; Carlberg, C. Different molecular mechanisms of vitamin D(3) receptor antagonists. *Mol. Pharmacol.* **2001**, *59*, 1478–1485.

(35) Ishizuka, S.; Kurihara, N.; Reddy, S. V.; Cornish, J.; Cundy, T.; Roodman, G. D. (23S)-25-Dehydro-1α-hydroxyvitamin D3−26,23-lactone, a vitamin D receptor antagonist that inhibits osteoclast formation and bone resorption in bone marrow cultures from patients with Paget's disease. *Endocrinology* **2005**, *146*, 20232030.

(36) Miura, D.; Manabe, K.; Ozono, K.; Saito, M.; Gao, Q.; Norman, A. W.; Ishizuka, S. Antagonistic action of novel 1α,25-dihydroxyvitamin D3−26, 23-lactone analogs on differentiation of human leukemia cells (HL-60) induced by 1α,25-dihydroxyvitamin D3. *J. Biol. Chem.* **1999**, *274*, 16392–16399.

(37) Fujishima, T.; Kojima, Y.; Azumaya, I.; Kittaka, A.; Takayama, H. Design and synthesis of potent vitamin D receptor antagonists with A-ring modifications: remarkable effects of 2α-methyl introduction on antagonistic activity. *Bioorg. Med. Chem.* **2003**, *11*, 3621–3631.

(38) Kato, Y.; Nakano, Y.; Sano, H.; Tanatani, A.; Kobayashi, H.; Shimazawa, R.; Koshino, H.; Hashimoto, Y.; Nagasawa, K. Synthesis of 1α,25-dihydroxyvitamin D3−26,23-lactams (DLAMs), a novel series of 1α,25-dihydroxyvitamin D3 antagonist. *Bioorg. Med. Chem. Lett.* **2004**, *14*, 2579–2583.

(39) Yoshimoto, N.; Inaba, Y.; Yamada, S.; Makishima, M.; Shimizu, M.; Yamamoto, K. 2-Methylene 19-nor-25-dehydro-1α-hydroxyvitamin D3 26,23-lactones: synthesis, biological activities, and molecular basis of passive antagonism. *Bioorg. Med. Chem.* **2008**, *16*, 457–473.

(40) Ma, Y.; Khalifa, B.; Yee, Y. K.; Lu, J.; Memezawa, A.; Savkur, R. S.; Yamamoto, Y.; Chintalacharuvu, S. R.; Yamaoka, K.; Stayrook, K. R.; Bramlett, K. S.; Zeng, Q. Q.; Chandrasekhar, S.; Yu, X.-P.; Linebarger, J. H.; Iturria, S. J.; Burris, T. P.; Kato, S.; Chin, W. W.; Nagpal1, S. Identification and characterization of noncalcemic, tissue-selective, nonsecosteroidal vitamin D receptor modulators. *J. Clin. Invest.* **2006**, *116*, 892–904.

(41) Rochel, N.; Wurtz, J. M.; Mitschler, A.; Klaholz, B.; Moras, D. The crystal structure of the nuclear receptor for vitamin D bound to its natural ligand. *Mol. Cell* **2000**, *5*, 173–179.

(42) Tocchini-Valentini, G.; Rochel, N.; Wurtz, J. M.; Mitschler, A.; Moras, D. Crystal structures of the vitamin D receptor complexed to superagonist 20-epi ligands. *Proc. Natl. Acad. Sci. U.S.A.* **2001**, *98*, 5491–5496.

(43) Vanhooke, J. L.; Benning, M. M.; Bauer, C. B.; Pike, J. W.; DeLuca, H. F. Molecular structure of the rat vitamin D receptor ligand binding domain complexed with 2-carbon-substituted vitamin D(3) hormone analogues and a LXXLL-containing coactivator peptide. *Biochemistry* **2004**, *43*, 4101–4110.

(44) Tocchini-Valentini, G.; Rochel, N.; Wurtz, J. M.; Moras, D. Crystal structures of the vitamin D nuclear receptor liganded with the vitamin D side chain analogues calcipotriol and seocalcitol, receptor agonists of clinical importance. Insights into a structural basis for the switching of calcipotriol to a receptor antagonist by further side chain modification. *J. Med. Chem.* **2004**, *47*, 1956–1961.

(45) Eelen, G.; Verlinden, L.; Rochel, N.; Claessens, F.; De Clercq, P.; Vandewalle, M.; Tocchini-Valentini, G.; Moras, D.; Bouillon, R.; Verstuyf, A. Superagonistic action of 14-epi-analogs of 1,25-dihydroxyvitamin D explained by vitamin D receptor-coactivator interaction. *Mol. Pharmacol.* **2005**, *67*, 1566–1573.

(46) Hourai, S.; Fujishima, T.; Kittaka, A.; Suhara, Y.; Takayama, H.; Rochel, N.; Moras, D. Probing a water channel near the A-ring of receptor-bound 1α,25-dihydroxyvitamin D3 with selected 2α-substituted analogues. *J. Med. Chem.* **2006**, *49*, 5199–5205.

(47) Ciesielski, F.; Rochel, N.; Moras, D. Adaptability of the vitamin D nuclear receptor to the synthetic ligand gemini: remodeling the LBP with one side chain rotation. *J. Steroid Biochem. Mol. Biol.* **2007**, *103*, 235–242.

(48) Vanhooke, J.; Tadi, B. P.; Benning, M. M.; Plum, L. A.; DeLuca, H. F. Crystal structure of the vitamin D nuclear receptor ligand binding domain in complex with a locked side chain analog of calcitriol. *Arch. Biochem. Biophys.* **2007**, *460*, 161–165.

(49) Rochel, N.; Hourai, S.; Rerez-Garcia, X.; Rumbo, A.; Mourino, A.; Moras, D. Crystal structure of the vitamin D nuclear receptor ligand binding domain in complex with a locked side chain analog of calcitriol. *Arch. Biochem. Biophys.* **2007**, *460*, 172–176.

(50) Yamamoto, K.; Abe, D.; Yoshimoto, N.; Choi, M.; Yamagishi, K.; Tokiwa, H.; Shimizu, M.; Makishima, M.; Yamada, S. Vitamin D receptor: ligand recognition and allosteric network. *J. Med. Chem.* **2006**, *49*, 1313–1324.

(51) Igarashi, M.; Yoshimoto, N.; Yamamoto, K.; Shimizu, M.; Ishizawa, M.; Makishima, M.; DeLuca, H. F.; Yamada, S. Identification of a highly potent vitamin D receptor antagonist: (25S)-26-adamantyl-25-hydroxy-2-methylene-22,23-didehydro-19,27-dinor-20-epi-vitamin D3 (ADMI3). *Arch. Biochem. Biophys.* **2007**, *460*, 240–253.

(52) Yoshimoto, N. Vitamin D Receptor Antagonists: Design, Synthesis, Biological Activities, and Molecular Basis of Antagonism. Thesis, Tokyo Medical and Dental University, 2008.

(53) Inaba, Y.; Yamamoto, K.; Yoshimoto, N.; Matsunawa, M.; Uno, S.; Yamada, S.; Makishima, M. Vitamin D3 derivatives with adamantane or lactone ring side chains are cell type-selective vitamin D receptor modulators. *Mol. Pharmacol.* **2007**, *71*, 1298–1311.

(54) Sicinski, R. R.; Prahl, J. M.; Smith, C. M.; DeLuca, H. F. New 1α,25-dihydroxy-19-norvitamin D3 compounds of high biological activity: synthesis and biological evaluation of 2-hydroxymethyl, 2-methyl, and 2-methylene analogues. *J. Med. Chem.* **1998**, *41*, 4662–4674.

(55) Shevde, N. K.; Plum, L. A.; Clagett-Dame, M.; Yamamoto, H.; Pike, J. W.; DeLuca, H. F. A potent analog of 1α,25-dihydroxyvitamin D3 selectively induces bone formation. *Proc. Natl. Acad. Sci. U.S.A.* **2002**, *99*, 13487–13491.

(56) Otwinowski, Z.; Minor, W. Processing of X-ray diffraction data collected in oscillation mode. *Methods Enzymol.* **1997**, *276*, 307–326.

(57) Brünger, A. T.; Adams, P. D.; Clore, G. M.; DeLano, W. L.; Gros, P.; Grosse-Kunstleve, R. W.; Jiang, J.-S.; Kuszewski, J.; Nilges, M.; Pannu, N. S.; Read, R. J.; Rice, L. M.; Simonson, T.; Warren, G. L. Crystallography & NMR system: a new software suite for macromolecular structure determination. *Acta Crystallogr.* **1998**, *D54*, 905–921.

(58) McRee, D. E. XtalView/Xfit—a versatile program for manipulating atomic coordinates and electron density. *J. Struct. Biol.* **1999**, *125*, 156–165.

(59) The Protein Data Bank accession numbers for the coordinates of the structures of the VDR complexes with (25*R*)-25-adamantyl-1α,25-hydroxy-2-methylene-22,23-didehydro-19,26,27-trinor-20-epivitamin $D_3$ (**2a**), (24*R*)-24-adamantyl-1α,24-hydroxy-2-methylene-22,23-didehydro-19,25,26,27-tetranor-vitamin $D_3$ (**2b**), (25*R*)-26-adamantyl-1α,25-hydroxy-2-methylene-22,23-didehydro-19,27-dinor-20-epivitamin $D_3$ (**2c**), and 1,25$(OH)_2D_3$ (**1**) reported in this article are 2ZMI, 2ZMH, 2ZMJ, and 2ZLC, respectively.

JM8004477